PHYSICAL REVIEW B **77**, 220101(R) (2008)

Proton radiography and accurate density measurements: A window into shock wave processes

P. A. Rigg,* C. L. Schwartz, R. S. Hixson, G. E. Hogan, K. K. Kwiatkowski, F. G. Mariam, M. Marr-Lyon, F. E. Merrill, C. L. Morris, P. Rightly, A. Saunders, and D. Tupa
Los Alamos National Laboratory, Los Alamos, New Mexico 87545, USA

(Received 4 February 2008; published 5 June 2008)

Direct density measurements were made from shock-loaded aluminum and copper samples by combining plate-impact experiments with proton radiography at the Los Alamos Neutron Science Center. Flyer plates were accelerated using a 40 mm bore powder gun to create a shock wave in a sample. The sample material was then interrogated in real time using the proton radiography facility. The increase in density behind the shock front causes a measurable change in the transmission of protons through the sample, which can then be quantified as a density value in the material. Hugoniot values were calculated using more traditional techniques to evaluate the accuracy of the radiographically obtained density measurements.

DOI: 10.1103/PhysRevB.77.220101 PACS number(s): 62.50.Ef, 64.30.Ef, 81.70.Bt, 06.30.Dr

I. INTRODUCTION

Accurate equations of state (EOS) are required for high fidelity simulations of dynamic processes. Applications are broad and there is a premium on accuracy and precision. In particular, knowledge of density at extreme conditions of stress and strain rate is important to such simulations. Physics-based material models are often very sensitive to the relationship between stress and density. However, methods to directly measure density in real time in a shock-compression experiment have been lacking. Therefore, measurement of other quantities, experimentally, is necessary to calculate the density in the shocked state. These calculations are themselves very sensitive to errors in other measured quantities, making it extremely difficult to obtain precise (better than 1%) determinations of density. In this paper, we describe the ability to measure density directly in shock-compressed materials with high accuracy using proton radiography.

The ability to obtain radiographs of dynamic events on the nano- or microsecond time scale using protons is a relatively new development[1] at Los Alamos National Laboratory. In the past, x radiography has been used to directly observe phase transition waves[2] or dynamic damage processes[3] but such techniques were not used to quantify density. There are three main advantages to using protons created with the Los Alamos Neutron Science Center's (LANSCE) 800 MeV linear accelerator for radiography over x rays. First, x-ray radiographs often suffer from parallax, creating a somewhat blurred image. Improvements to this condition can be made by minimizing source to detector distance or collimating the beam, which is not always practical. However, since protons are charged particles, magnetic "lenses" can be used to create much sharper flash radiographic images than x rays. Second, the 1 ms long proton pulse created at LANSCE can be chopped into 50 ns wide pulses spaced several hundred nanoseconds apart. This allows multiple frames of radiographic data to be obtained with precise timing between frames. Finally, the signal to noise ratio, or contrast, is typically much higher with proton radiography, making determination of density more tractable than with x radiography.

II. EXPERIMENT METHOD

Although proton radiography data have been obtained, which are of general interest to the physics community,[1] specific experiments to produce quantitative measurements of the density of shock-compressed metals have not been done. To address this important need, we have designed and built a 40 mm bore powder-driven gun to launch planar flyer plates up to velocities of 1.8 km/s and coupled it to the LANSCE proton beam. Plate impact experiments using gas- and powder-driven guns are well suited to investigate dynamic compression of solids because they produce well-characterized one-dimensional loading in shocked samples.[4] Synchronization of the shock event—which lasts for only a few microseconds—to a single proton pulse window was achieved in two stages. First, the total system time of the gun ($\sim$10 ms) was made to be reproducible to $\pm$150 μs to ensure that the impact would occur during the active part of the proton accelerator duty cycle, a 1 ms gate occurring at 120 Hz. This was achieved using an electrically fired, low-jitter detonator to initiate the powder burn and the placement of a shear disk on the back of the projectile. This shear disk functioned like a burst diaphragm to prevent premotion of the projectile before full burn of the powder could be achieved. Second, a proton "chopper" was activated using a trigger pin placed 12 mm from the target to send a tailored sequence of proton "micropulses" 50 ns long and 400 ns apart to the target chamber of the gun at the time of flyer plate impact.

6061-T6 aluminum and oxygen free high conductivity (OFHC) copper were chosen for the initial experiments because of the large body of shock wave data that exists on these two materials. Existing material models have proven effective in describing the dynamic response of both 6061-T6 Al (Refs. 5 and 6) and OFHC Cu (Ref. 7) when subjected to one-dimensional shock wave loading. Therefore, provided that the projectile velocity was measured during the experiment, the final density in the shocked state could be calculated with a high degree of confidence and compared directly to the density measurements obtained from the radiographs.

The experimental configuration used to obtain radiographic data from shocked samples is shown schematically

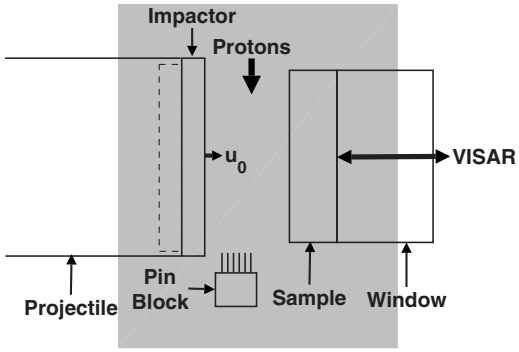

FIG. 1. Representation of the experimental configuration used. The pin block was used to both trigger the chopper and measure the projectile velocity.

in Fig. 1. Impactors of aluminum and copper were accelerated to velocities of ~1.45 and ~1.25 km/s, respectively, and impacted on samples of the same material. In this "symmetric impact" configuration, conservation of momentum dictates that the in-material particle velocity is equal to one-half of the projectile velocity. This technique is often used to obtain Hugoniot data from uncharacterized materials[8] but is used here to reduce uncertainties in the calculated final densities in each experiment. The samples and impactors were 38 and 40 mm in diameter, respectively, and nominally 12 mm thick. Samples were backed by LiF[100] windows to preserve the shocked state in the sample for as long as possible and maximize our chances of successful synchronization of the proton beam to the shock event. In the aluminum experiments, shock propagation through the sample takes just under 2 μs and just over 2 μs in the copper experiments. In each experiment, at least two radiographs were obtained to quantitatively measure the material density behind the shock front.

III. EXPERIMENT RESULTS

A summary of all four experiments performed in this series is shown in Table I. Iimpactor velocities were determined using data obtained from six electrical shorting pins (24 V_{DC} bias) placed in line to the projectile direction of motion and 2 mm apart, the first of which was used to trigger the proton chopper as mentioned above (see Fig. 1). Uncertainties were determined from a statistical analysis of the pin data. Initial densities of the materials used were determined by measuring the mass and volume (water displacement technique) of multiple samples from the same starting material multiple times. The final stress for each experiment was then calculated using the known relationships between the stress and particle velocity for aluminum[5,6] and copper.[7] For aluminum, the relationship

$$P = 0.1184 + 14.02u_p + 3.738u_p^2 \tag{1}$$

was used and for copper,

$$P = 35.18u_p + 13.30u_p^2 \tag{2}$$

was used. The Rankine–Hugoniot jump conditions[9] for conservation of mass and momentum,

$$\rho = \frac{\rho_0 U_s}{U_s - u_p}, \tag{3}$$

and

$$P = \rho_0 U_s u_p, \tag{4}$$

were then used to calculate the final density in the shocked state. Here, ρ and P are the final density and stress, respectively, and ρ_0, U_s, and u_p are the initial density, shock velocity, and particle velocity, respectively. A simple substitution to eliminate U_s in Eq. (3) leads to

$$\rho = \frac{\rho_0 P}{P - \rho_0 u_p^2}. \tag{5}$$

The uncertainty for all calculated values of stress and density were determined using the error analysis approach outlined by Mitchell and Nellis.[8]

Protons transmitted through the target were imaged using an electromagnetic lens constructed of four quadrupole magnets[10] and a tiled array of thin lutetium oxyorthosilicate (LSO) scintillators.[11] The light produced by individual pulses of protons was relayed through a mirror and lens system, and imaged with a set of fast-gated charge-coupled device cameras.[12] Each camera was gated in sequence to coincide with a single proton micropulse.

TABLE I. Summary of the experiments with the uncertainties for each quantity shown in parentheses.

Experiment	Impactor/ sample	Impactor velocity (mm/μs)	Peak stress (GPa)	Initial density (g/cm^3)	Calculated density (g/cm^3)	Measured density (g/cm^3)	Agreement
1	Al 6061-T6	1.452	12.27	2.710	3.067	3.070	0.1%
		(0.012)	(0.11)	(0.003)	(0.005)	(0.025)	
2	Al 6061-T6	1.422	11.98	2.710	3.060	3.056	0.1%
		(0.002)	(0.03)	(0.003)	(0.004)	(0.020)	
3	OFHC Cu	1.30	28.59	8.928	10.30	10.28	0.2%
		(0.04)	(0.91)	(0.003)	(0.05)	(0.08)	
4	OFHC Cu	1.249	27.16	8.928	10.241	10.28	0.4%
		(0.002)	(0.06)	(0.003)	(0.006)	(0.08)	

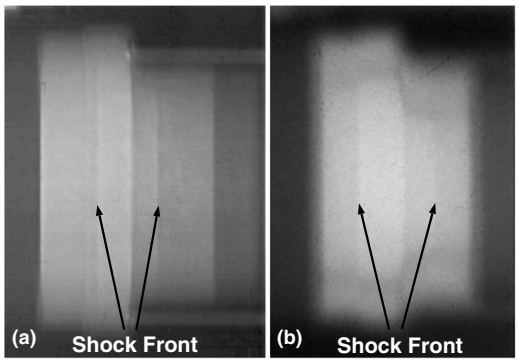

FIG. 2. Single radiographic frames obtained from (a) experiment 1 and (b) experiment 3, showing the progression of the shock front roughly one-third and one-half of the way through the sample, respectively.

The transmission of protons through the lens could be adjusted using a collimator to define the angular acceptance of the lens by removing protons scattered to large angles. Nuclear scattering and multiple Coulomb scattering are the two main components that attenuate the protons through the target. Protons that nuclear scatter outside of the energy acceptance of the magnetic lens and protons that multiple Coulomb scatter outside the angular acceptance of the collimator are removed. Approximating these two components leads to transmission t through a target of thickness l, of the form,

$$t = e^{-1/\lambda}(1 - e^{-X/l}), \tag{6}$$

where λ parameterizes the attenuation due to nuclear scattering and X parameterizes the attenuation due to multiple Coulomb scattering. The parameters needed for this model were fitted to transmission data taken from static measurements of the aluminum and copper targets before the dynamic experiment.

Single radiographic frames from experiments 1 and 3 are shown in Fig. 2. Here, darker pixels represent higher proton transmission and, thus, lower density. Due to the cylindrical shape of the samples, the top and bottom of the sample are much thinner than the middle with respect to proton transmission. This causes significant distortions of the images in experiment 3 [Fig. 2(b)] but did not affect the density measurement at the center of the sample. Attempts to reduce these distortions, caused by protons scattering within the sample, were made in experiment 4 but did not improve the results. Distortions are not seen in the aluminum images because the initial density is relatively low.

As the shock propagates longitudinally in the sample, edge release waves propagate radially in toward the center of the sample; thus, protons pass through both one-dimensionally shocked and edge-released material in every frame. To obtain accurate measurements of density from the radiographs, the effect of these edge release waves must be accounted for. To do this, a tomographic reconstruction was calculated using a regularized-Abel inversion of the edge-released portion of the radiograph. A forward model was then applied to produce a simulated areal radiograph of the edge-released material alone. Finally, this simulated radiograph was subtracted from the experimental radiograph to produce a corrected areal density radiograph of the shocked and unshocked material with the edge-released portion removed. An illustration of this process is shown in Fig. 3. Density values were obtained from this corrected areal density radiograph by measuring the transmission of the protons in the unshocked and shocked states using Eq. (6). The transmission of protons through the unshocked material could then be referenced to the measured density of the material in the unshocked state (see Table I) to determine the density of the shocked material directly.

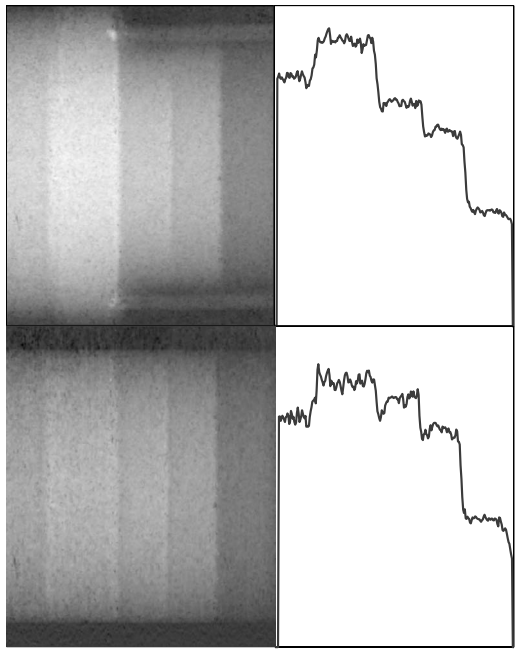

FIG. 3. (a) Areal and (b) corrected areal density radiographs for experiment 1 with lineouts shown to the right for both images. Note that this radiograph was obtained 400 ns after the radiograph shown in Fig. 2(a).

The shocked densities measured from the radiographs for all experiments are listed in Table I. Five static radiographs of the target were analyzed to determine the uncertainty in the density. These were processed in the same manner as the dynamic experiment producing areal densities for the target with similar statistical and systematic errors, as are observed in the dynamic experiment, but for a cylinder of material with known constant density. The ratios of densities were calculated on either side of an assumed edge for a number of independent trials. The standard deviation of these trials was taken as the density uncertainty for the dynamic experiment. However, since the density was calculated for each experiment with quantifiable uncertainties, the measured and calculated values could be compared directly. This is shown both in Table I and Fig. 4. As can be seen in the final column of Table I, the agreement is better than 0.5% for all measurements, indicating that the density measurement error may be smaller than can be determined using the technique described above. This is largely due to the statistical noise present in each radiograph.

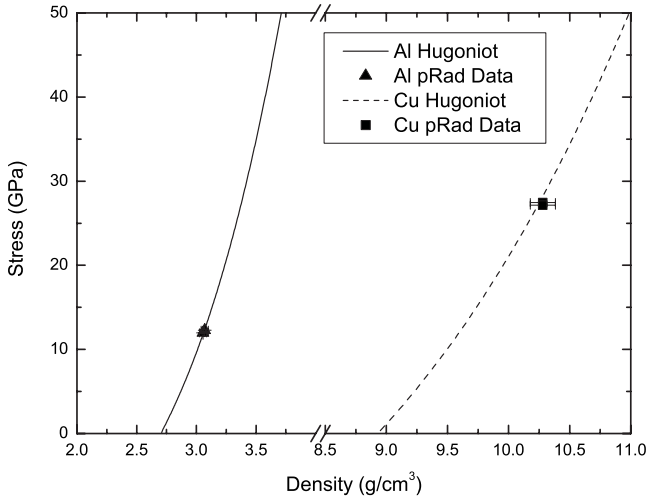

FIG. 4. Stress vs. density for aluminum (left) and copper (right) showing the agreement between the measured densities (with error bars) and the calculated Hugoniots for both materials.

IV. CONCLUSION

Quantitative, direct density measurements using proton radiography have been made in shock-compression experiments. The densities of metals shock compressed using the plate-impact technique have been directly determined to better than 1% accuracy with agreement to calculated values to better than 0.5%. Thus, changes in density as small as 2%–3% are expected to be resolvable using this technique. Experiments were performed on two materials with well-known equations of state but with largely different initial densities to demonstrate the range of materials to which this technique is applicable. Although image quality was reduced in the copper experiments, accurate measurements were nonetheless obtained showing broad applicability to materials with widely varying physical properties. Determining the shocked density of materials with much higher initial densities than copper—such as tantalum or tungsten—should also be possible provided that the diameter of the samples is made smaller to compensate. However, reducing the diameter of the sample also reduces the percentage of material in uniaxial strain due to the propagation of edge release waves. Therefore, care must be taken in balancing the reduction of diameter and consequential increase in contrast to obtain the highest fidelity measurements possible. This will be a focus area of the authors for future experiments.

The ability to obtain accurate direct density measurements in a plate-impact experiment should prove useful in the development of robust equations of state for many materials. In particular, materials that undergo shock-induced solid–solid and solid–liquid phase transformations are of general interest. Materials such as iron, which transforms from the α (fcc) to ϵ (bcc) structure at 13 GPa,[13] and tin, which will melt when released from a stress of 23 GPa,[14] will be the subject of future experiments. For iron, a single, correctly-timed snapshot should provide an accurate density measurement of the α phase shocked to the transition stress and the ϵ phase shocked to the peak stress of the experiment. In addition, multiple snapshots should provide shock velocities for both phases. Such information can be used to confirm or refine our multiphase equation of state for iron and may provide better insight into these phenomena.

ACKNOWLEDGMENTS

We would like to thank Dennis Shampine, Mark Byers, and Frank Abeyta for their tireless efforts to design, build, and characterize the 40 mm gun. We would also like to thank the pRad team for the expertise and long hours put in to make these experiments successful. Finally, we would like the thank the LANSCE operations crew for the quality and reliable beam delivery.

*prigg@lanl.gov

[1] C. Morris, J. W. Hopson, and P. Goldstone, Los Alamos Sci. **30**, 32 (2006).

[2] B. R. Breed and D. Venable, J. Appl. Phys. **39**, 3222 (1968).

[3] C. L. Mader, T. R. Neal, and R. D. Dick, *LASL PHERMEX Data* (University of California Press, Berkeley, 1980), Vol. I.

[4] G. R. Fowles, G. E. Duvall, J. Asay, P. Bellamy, F. Feistmann, D. Grady, T. Michaels, and R. Mitchell, Rev. Sci. Instrum. **41**, 984 (1970).

[5] C. D. Lundergan and W. Herrmann, J. Appl. Phys. **34**, 2046 (1963).

[6] W. M. Isbell and D. R. Christman, Techical Report No. MSL-69-60, General Motors, 1970 (unpublished).

[7] R. G. McQueen, S. P. Marsh, J. W. Taylor, J. N. Fritz, and W. J. Carter, *High Velocity Impact Phenomena* (Academic, New York, 1970).

[8] A. C. Mitchell and W. J. Nellis, J. Appl. Phys. **52**, 3363 (1981).

[9] See, for example, R. Courant and K. O. Friederichs, *Supersonic Flow and Shock Waves* (Interscience, New York, 1948).

[10] C. T. Mottershead and J. D. Zumbro, in Proceedings of the 17th Particle Accelerator Conference, edited by M. Comyn, M. Craddock, M. Reiser, and J. Thomson (IEEE, Vancouver, Canada, 1998).

[11] K. Kwiatkowski, N. S. P. King, and V. M. Douence, Los Alamos Sci. **30**, 46 (2006).

[12] N. S. P. King, S. Baker, S. Jaramillo, K. Kwiatkowski, S. Lutz, G. E. Hogan, V. Holmes, C. L. Morris, P. Nedrow, P. D. Pazuchanics, J. Rohrer, D. Sorenson, and R. Thompson, in Proc. SPIE **4948**, 610 (2003).

[13] D. Bancroft, E. L. Peterson, and S. Minshall, J. Appl. Phys. **27**, 291 (1956).

[14] C. Mabire and P. L. Hèreil, in *Shock Compression of Condensed Matter — 1999*, edited by M. D. Furnish, L. C. Chhabildas, and R. S. Hixson (AIP, Melville, New York, 1999).